Science of the Total Environment 765 (2021) 144385

Contents lists available at ScienceDirect

Science of the Total Environment

journal homepage: www.elsevier.com/locate/scitotenv

Modelling CO_2 and CH_4 emissions from drained peatlands with grass cultivation by the BASGRA-BGC model

Xiao Huang [a,*], Hanna Silvennoinen [b], Bjørn Kløve [c], Kristiina Regina [d], Tanka P. Kandel [e], Arndt Piayda [f], Sandhya Karki [g], Poul Erik Lærke [h], Mats Höglind [a]

[a] *Norwegian Institute of Bioeconomy Research, Klepp Station, Norway*
[b] *Norwegian Institute of Bioeconomy Research, Ås, Norway*
[c] *Water, Energy and Environmental Engineering Research Unit, University of Oulu, Oulu, Finland*
[d] *Bioeconomy and Environment Unit, Natural Resources Institute Finland, Jokioinen, Finland*
[e] *Noble Research Institute, LLC, Ardmore, USA*
[f] *Thünen Institute for Climate-Smart Agriculture, Braunschweig, Germany*
[g] *Delta Water Management Research Unit, USDA-ARS, Jonesboro, USA*
[h] *Department of Agroecology, Aarhus University, Interdisciplinary Centre for Climate Change, Tjele, Denmark*

HIGHLIGHTS

- Dual-porosity framework is used for the soil properties of drained peatlands.
- Model outputs represent the trade-offs between CO_2 and CH_4 under different WTLs.
- SOM decomposition rate could vary significantly under the same WTLs.
- This model can be used to optimize water table management for drained peatlands.

GRAPHICAL ABSTRACT

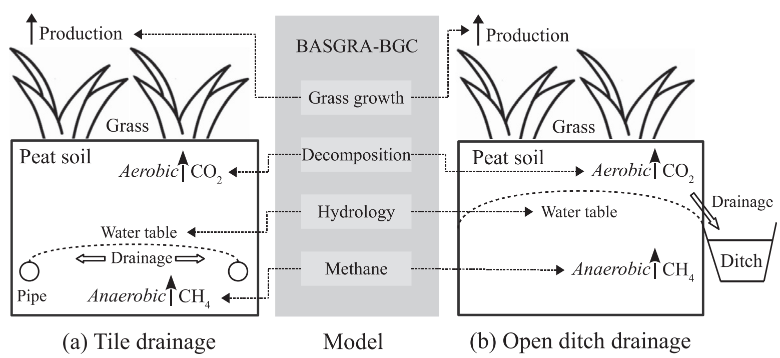

ARTICLE INFO

Article history:
Received 27 September 2020
Received in revised form 11 November 2020
Accepted 4 December 2020
Available online 25 December 2020

Editor: Jurgen Mahlknecht

Keywords:
Cultivated peatlands
Drainage
WTL
CO_2
CH_4
BASGRA-BGC model

ABSTRACT

Cultivated peatlands under drainage practices contribute significant carbon losses from agricultural sector in the Nordic countries. In this research, we developed the BASGRA-BGC model coupled with hydrological, soil carbon decomposition and methane modules to simulate the dynamic of water table level (WTL), carbon dioxide (CO_2) and methane (CH_4) emissions for cultivated peatlands. The field measurements from four experimental sites in Finland, Denmark and Norway were used to validate the predictive skills of this novel model under different WTL management practices, climatic conditions and soil properties. Compared with daily observations, the model performed well in terms of *RMSE* (Root Mean Square Error; 0.06–0.11 m, 1.22–2.43 gC/m^2/day, and 0.002–0.330 kgC/ha/day for WTL, CO_2 and CH_4, respectively), *NRMSE* (Normalized Root Mean Square Error; 10.3–18.3%, 13.0–18.6%, 15.3–21.9%) and *Pearson's r* (Pearson correlation coefficient; 0.60–0.91, 0.76–0.88, 0.33–0.80). The daily/seasonal variabilities were therefore captured and the aggregated results corresponded well with annual estimations. We further provided an example on the model's potential use in improving the WTL management to mitigate CO_2 and CH_4 emissions while maintaining grass production. At all study sites, the simulated WTLs and carbon decomposition rates showed a significant negative correlation. Therefore, controlling WTL could effectively reduce carbon

* Corresponding author.
E-mail address: xiao.huang@nibio.no (X. Huang).

https://doi.org/10.1016/j.scitotenv.2020.144385

losses. However, given the highly diverse carbon decomposition rates within individual WTLs, adding indicators (e.g. soil moisture and peat quality) would improve our capacity to assess the effectiveness of specific mitigation practices such as WTL control and rewetting.

1. Introduction

Northern peatlands sequester carbon dioxide (CO_2) effectively (Yu, 2012). With waterlogged and anaerobic conditions, they are also significant sources of methane (CH_4) to the atmosphere (Harriss et al., 1985; Smith et al., 2004). In the Nordic countries, peat soils are important for agriculture, accounting for about 2.0% (Nielsen et al., 2013), 7.0% (Kløve et al., 2010), 8.7% (Berglund and Berglund, 2010) and 10.4% (Myllys et al., 2012) of the total agriculture area in Denmark, Norway, Sweden and Finland, respectively. Cultivated peatlands in this region are extensively drained for crop growth and grasslands of animal husbandry in particular (Kasimir et al., 2018). However, drainage accelerates the soil organic carbon (SOC) decomposition by introducing more oxygen into the soil, thus shifting the peatlands from C sinks into significant sources of CO_2 (Grønlund et al., 2008). Assessing greenhouse gas (GHG) emissions from cultivation practices is important in the Nordic countries as they make efforts to realize their goals for both improved food security (Forbord and Vik, 2017) and mitigation of GHG emissions (e.g. EU's 2030 climate & energy framework to cut at least 40% GHG emissions). In the future, prolonged growing seasons in boreal regions may provide opportunities for agricultural development (Wiréhn, 2018), while warmer and drier soil environment could further increase SOC decomposition. With increase temperature and droughts peatlands can secure grass production, but their carbon stocks will be more vulnerable. Due to the high emission rate, mitigating emissions from drained peatland could be an effective option to tackle climate change (Leifeld and Menichetti, 2018) compared to the C sequestration strategies for mineral soils as suggested by the 4‰ initiative of the Lima Paris Action Agenda (Chabbi et al., 2017). Consequently, finding environment-friendly management practices for drained peatlands is of great importance for the Nordic agriculture (Kløve et al., 2017).

Estimation of annual GHG emissions using data from field experiments on cultivated peatlands (Berglund and Berglund, 2011; Kløve et al., 2010; Maljanen et al., 2003; Regina and Alakukku, 2010) that are usually short in duration and have infrequent sampling, may fail to capture important feedbacks from management practices. Modelling methods have been established to simulate the biogeochemical processes of cultivated peatlands with higher spatio-temporal resolution than those available from field experiments. The empirical regression approaches (e.g. Kandel et al., 2017; Lloyd and Taylor, 1994), which directly build the relationship between GHG emission rate and certain measured variables, are popular tools for interpolating and upscaling the existing measurements (Eickenscheidt et al., 2015; Karki et al., 2019; Lohila et al., 2003). Such data-driven methods, however, could be limited in integrating complex environmental factors to predict optimal management schemes.

On the other hand, process-based models describe the interactions between plants and soil environment in more detail than the empirical regression approaches. These models, including biogeochemical models (Frolking et al., 2001; Kleinen et al., 2012; Mezbahuddin et al., 2016), global vegetation models (Wania et al., 2009) and land surface models (Qiu et al., 2018; Qiu et al., 2019; Shi et al., 2015), have been developed to simulate the C dynamics of Northern peatlands. However, we identified three key challenges for current process-based models related to the modelling of biogeochemical processes of the cultivated peatlands with grass cultivation in the Nordic region: (i) While grass cultivation accounts for the highest fraction of cultivated peatlands in this region, most of the current models with specially developed peat soil module (e.g. Orchidee-Peat, CLIMBER2-LPJ) mainly focus on forest ecosystems. As the interaction between plants and soil largely controls the GHG emissions and C balance, a proper module simulating the grass growth and its winter survival in the Northern environment is needed; (ii) Unlike pristine peatlands with relatively stable water table level (WTL), cultivated peatlands exhibit obvious WTL variations due to drainage and climate. A detailed hydrological module with higher temporal resolution than seasonal or annual step is needed considering the specific properties of drained peat soils; (iii) Lack of corresponding modelling for different drainage and irrigation practices restricts model applications for exploring management effects on the GHG emissions.

To address these challenges, we developed the new model version BASGRA-BGC (BASic GRAss model – BioGeoChemical Cycle). The model specifically simulates the C balance, including CO_2 and CH_4 emissions, and biomass productivity, from drained peatlands with grass cultivation. The original BASGRA model is a process-based model for simulating the daily-step dynamics of leaves, roots, tillers and biomass (Höglind et al., 2016) with detailed processes for cold hardening and dehardening. The latest model version BASGRA_N also couples modules of N supply from soil and N allocation among plant organs (Höglind et al., 2020). BASGRA_N and its predecessor has been well validated for grass growth modelling in the Nordic region and used to investigate different schemes to improve grassland management including ideotype design and optimal fertilization (Hjelkrem et al., 2017; Korhonen et al., 2018; Van Oijen and Höglind, 2016; Woodward et al., 2020). We developed the BASGRA-BGC version based on BASGRA_N by coupling modules from SWAT, Century and DNDC models.

The objectives of this paper are to: (i) describe the new features of BASGRA-BGC which was developed to simulate WTL, CO_2 and CH_4 emissions from drained peatlands with grass cultivation; (ii) evaluate its performance for WTL, CO_2 and CH_4 prediction against data from field experiments in Finland, Denmark and Norway; (iii) use the model to propose improved drainage schemes to mitigate GHG emissions and maintain grass production.

2. Model development

BASGRA_N model, mainly focusing on the simulation of physiological processes of the above-ground grass growth, represents soil physical and biological processes in a rather simplistic way, which limits its capability to simulate the complex biogeochemical interactions characterizing cultivated peat soils. For example, in BASGRA_N the vertical soil column is represented as one single layer, and the current version does not simulate draining process and CH_4 emissions. Therefore, the new version BASGRA-BGC uses a multi-layer soil structure (user defined) for the vertical soil column with layer-dependent simulation of hydrological and biogeochemical processes, including CO_2 and CH_4 emissions. Detailed functions are described in the following Sections 2.1–2.3. The list of variable abbreviations used in this paper is provided in Table 1.

2.1. Hydrological processes

Compared with mineral soils, peat soils have a higher SOC content with lower bulk density and larger total porosity. The dominating macro-scale pores in undecomposed peat can actively transmit water to infiltration, evapotranspiration and drainage (Rezanezhad et al., 2016). However, for degraded peat with long drainage history, the plant debris is broken down into smaller fragments and a high proportion of large pores is therefore turned into small and closed pores

Table 1
Explanation of variable abbreviations.

Name	Description	Unit	Equation
State variable			
$SW_{m,i}/SW_{im,i}$	The soil water content of mobile/immobile part in the *i*th soil layer	$mm \cdot H_2O$	(1a)/(1b)
$\theta_{m,i}/\theta_{im,i}$	The relative soil moisture in mobile/immobile part in the *i*th soil layer	mm/mm	(1c)
$Tsoil_{z,j}$	The soil temperature at depth z on the *j*th day of the year	°C	(5)
$\overline{T}_{air}$	The average annual air temperature	°C	(5)
T_{surf}	The surface temperature	°C	(5)[a]
$CLit_k$ (CP_k)	Litter carbon pool: k=1, labile pool; k=2, resistant pool	$g \cdot C/m^2$	(9)
$CSOM_k$ (CP_k)	Soil organic carbon pool: k=1, very labile pool; k=2, labile pool; k=3, passive pool	$g \cdot C/m^2$	(9)
NSH/NRT	The nitrogen content in shoot/root	$g \cdot N/m^2$	(11a)/(11b)[a]
$CST/CLV/CRT/CSTUB$	The carbon content in stem/leaf/root/stubble	$g \cdot C/m^2$	[a]
DOC	The dissolved organic carbon in the soil layer	$g \cdot C/m^2$	(15a)
H_2	The hydrogen content in each soil layer	$g \cdot H/m^2$	(15b)
anf	The anaerobic fraction in each soil layer	–	(12)
FC	The soil water content at field capacity in each soil layer	$mm \cdot H_2O$	(12)
SAT	The saturated soil water content in each soil layer	$mm \cdot H_2O$	(12)
Non-state variables			
$Wm_{m,i}/Wm_{im,i}$	The water melting rate in mobile/immobile part in the *i*th soil layer	$mm \cdot H_2O$/day	(1a)/(1b)
$Wf_{m,i}/Wf_{im,i}$	The water freezing rate in mobile/immobile part in the *i*th soil layer	$mm \cdot H_2O$/day	(1a)/(1b)
I_i	The water infiltration rate in the *i*th soil layer	$mm \cdot H_2O$/day	(2)
$E_{s,i}$	The actual soil evaporation rate in the *i*th soil layer	$mm \cdot H_2O$/day	(3)
$E_{t,i}$	The actual transpiration rate in the *i*th soil layer	$mm \cdot H_2O$/day	(4)
D_i	The drainage rate in the *i*th soil layer	$mm \cdot H_2O$/day	(1a)
Ex_i	The water flux from mobile part to immobile part in the *i*th soil layer	$mm \cdot H_2O$/day	(1c)
dz_i	The depth of the *i*th soil layer	mm	(1c)
$SW_{excess,i}$	The infiltrative volume of water in the *i*th soil layer	$mm \cdot H_2O$/day	(S2a)
TT	The travel time for infiltration	hr	(S2b)
$E_{s,lower,i}/E_{s,upper,i}$	The cumulative evaporation rate until the lower/upper boundary of the *i*th soil layer	$mm \cdot H_2O$/day	(S3a)
$E_{t,lower,i}/E_{t,upper,i}$	The cumulative transpiration rate until the lower/upper boundary of the *i*th soil layer	$mm \cdot H_2O$/day	(S4a)
df	The depth factor	–	(S5a)
D_{pot}	The potential draining rate	$mm \cdot H_2O$/day	(6)(7)(8)
m	The height from water table to draining pipes	mm	(6)
t	The height from water table to soil surface	mm	(7)
CF_k	The carbon flux leaving the *k*th carbon pool	$g \cdot C\ /m^2$/day	(9)
$CF_{hr,k}$	The heterotrophic flux from the decomposition of the *k*th carbon pool	$g \cdot C/m^2$/day	(10)
MR_{sh}/MR_{rt}	The maintenance respiration rate in shoot/root	$g \cdot C/m^2$/day	(11a)
GR_{sh}/GR_{rt}	The growth respiration rate in shoot/root	$g \cdot C/m^2$/day	[a]
$andec_k$	The anaerobic decomposition rate of the *k*th SOM carbon pool	$g \cdot C/m^2$/day	(13)
$RTdec$	The root exudation rate in each soil layer	$g \cdot C/m^2$/day	(14)
$CH_{4,p1}/CH_{4,p2}/CH_{4,p}$	The CH_4 production rate from DOC/H_2/total	$g \cdot C/m^2$/day	(16a)/(16b)/(16c)
$CH_{4,trans}$	The CH_4 transport rate	$g \cdot C/m^2$/day	(18)
θ_{rt}	The relative soil moisture in the root zone	–	(19)
$\theta_{rt,sat}$	The relative saturated soil moisture in the root zone	–	(19)
Parameter			
$coef_{ex}$	The coefficient for water flux between mobile and immobile parts	day^{-1}	(1c)
$coef_l$	The lag coefficient that represent the influence of the previous day's temperature	–	(5)
K_e	The effective lateral hydraulic conductivity	$mm \cdot H_2O$/day	(S6a)
d_e	The corrected height from draining pipes to soil bottom	mm	(S6b)
g	Dimensionless factor	–	(S7)
D_m	The maximum open ditch drainage rate	$mm \cdot H_2O$/day	(8)
D_s	Scaling coefficient for D_m	–	(8)
W_s	Scaling coefficient for maximum soil moisture	–	(8)
θ_s	Average soil porosity from water table to soil bottom	–	(8)
$r_{0,k}$	The maximum decomposition rate coefficient for the *k*th carbon pool	yr^{-1}	(9)
f_{total}	The combined decomposition scalar considering temperature, soil moisture and depth factors	–	(S9a)
rf_k	The respiration fractions of litter and SOM pools	–	(10)
$r_{m,sh}/r_{m,rt}$	The base maintenance respiration rate in shoot/root	$g \cdot C/g \cdot N$/day	(11a)/(11b)
$f_{m,t}$	The temperature scalar for maintenance respiration	–	(S11)
$r_{an,k}$	The maximum anaerobic decomposition rate coefficient for the *k*th SOM carbon pool	yr^{-1}	(13)
$f_{total,an}$	The combined anaerobic decomposition scalar considering temperature and depth factors	–	(S13b)
r_{RT}	The maximum exudation rate coefficient	day^{-1}	(14)
$CH_{4,DOC}/CH_{4,H2}$	The maximum rate of CH4 production from DOC/H_2	$g \cdot C/m^2$/day	(S16c)
km_{DOC}/km_{H2}	The half saturation constant for DOC/H_2	$g \cdot C/m^3$ $g \cdot H/m^3$	(16a)/(16b)
$CH_{4,oxid,max}$	The maximum oxidation rate of CH_4 in each soil layer	$g \cdot C/m^2$/day	(S17a)
$f_{total,oxid}$	The combined oxidation scalar considering temperature and depth factors	–	(S17b)
$f_p/f_e/f_d$	The coefficient of plant transport/bubble ebullition/diffusion	–	(S18)
K_{aer}	The coefficient of deficient aeration conditions	–	(19)
θ_{air}	The anaerobiosis point of relative water moisture	–	(19)
Input			
L	The distance between draining pipes	mm	(6)(7)
b	The height from soil surface to draining pipes	mm	(7)
r	The radius of draining pipes	mm	(7)

[a] Calculated from the original BASGRA_N model.

(Bragazza et al., 2009). As a result, we used a dual-porosity framework that includes both "mobile zone" where water can move easily and "immobile zone" where water movement is negligible to simulate the hydrological processes in drained peat soils (Binet et al., 2013; Rezanezhad et al., 2016). As shown in Fig. 1, the immobile zone can only exchange water and solution with the mobile part. The overall mass balance equations (one dimension) for soil water modelling are as follows:

$$\frac{dSW_{m,i}}{dt} = I_{i-1} + Wm_{m,i} - I_i - E_{s,i} - E_{t,i} - D_i - Wf_{m,i} + Ex_i \tag{1a}$$

$$\frac{dSW_{im,i}}{dt} = Wm_{im,i} - Wf_{im,i} - Ex_i \tag{1b}$$

$$Ex_i = coef_{ex} \cdot (\theta_{m,i} - \theta_{im,i}) \cdot dz_i \tag{1c}$$

In the BASGRA-BGC model, we used the methods from the SWAT (Soil & Water Assessment Tool) model (Arnold and Fohrer, 2005) to calculate (i) soil water infiltration (Eq. (2)); (ii) the partition of total soil evaporation and transpiration in each layer (Eqs. (3) & (4)); (iii) the soil temperature as well as the thawing/freezing processes (Eq. (5)). We present the key functions in the main text and refer to the supplementary material for a full description of the detailed processes. Based on Eq. (5), the soil temperature at the center of each soil layer is computed and then linearly interpolated to get the soil temperature at any depth within the whole soil column. We assumed that the corresponding soil water in each soil layer is uniformly distributed and that the water within soil depth with below-zero temperature gets frozen.

Infiltration rate:

$$I_i = SW_{excess,i} \cdot \left(1 - exp\left(\frac{-24.0}{TT}\right)\right) \tag{2}$$

Soil evaporation rate:

$$E_{s,i} = E_{s,lower,i} - E_{s,upper,i} \tag{3}$$

Transpiration rate:

$$E_{t,i} = E_{t,lower,i} - E_{t,upper,i} \tag{4}$$

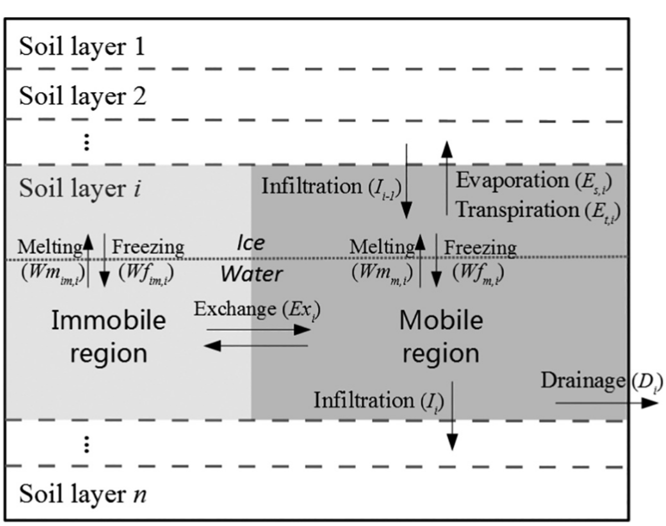

Fig. 1. The dual-porosity framework for hydrological modelling in the BASGRA-BGC model.

Soil temperature:

$$Tsoil_{z,j} = coef_l \cdot Tsoil_{z,j-1} + (1.0 - coef_l) \cdot (df \cdot (\overline{T}_{air} - T_{surf}) + T_{surf}) \tag{5}$$

Subsurface drainage is a popular practice in the Nordic region to lower the WTL of peatlands (Kløve et al., 2017). Tile drainage (here refers to subsurface drainage using tile, PVC pipe and other materials) together with open ditch is a common way to extensively drain the peatland while open ditch drainage only without pipe is another option which is less frequently used in this region. In BASGRA-BGC, the Hooghoudt (1940) steady-state (Eq. (6)) and Kirkham (1957) tile (Eq. (7)) equations are used to simulate the tile drainage flux with WTL below and above the soil surface. For open ditch drainage, we use the conceptual Arno model formulation (Franchini and Pacciani, 1991) to model the baseflow into the nearby ditch (Eq. (8)). After the potential drainage flux has been calculated, the actual drainage rate D_i in each layer is computed from the water table surface until the bottom layer to meet the total drainage potential.

Tile drainage with water table below soil surface:

$$D_{pot} = \frac{8K_e d_e m + 4K_e m^2}{L^2} \tag{6}$$

Tile drainage with water table above soil surface:

$$D_{pot} = \frac{4\pi K_e \cdot (t + b - r)}{gL} \tag{7}$$

Open ditch drainage:

$$D_{pot} = \begin{cases} \frac{D_s D_m}{W_s \theta_s} \cdot \theta, & \theta \le W_s \theta_s \\ \frac{D_s D_m}{W_s \theta_s} \cdot \theta + D_m \cdot \left(1 - \frac{D_s D_m}{W_s}\right) \cdot \left(\frac{\theta - W_s \theta_s}{\theta_s - W_s \theta_s}\right)^2, & \theta > W_s \theta_s \end{cases} \tag{8}$$

2.2. Soil decomposition and plant respiration

The decomposition of litter material and soil organic matter (SOM) is modelled using the Century-based cascade method (first-order decay model) between different carbon pools (Parton, 1996). We define two litter pools and three SOM carbon pools (see Table 1). The detailed routines of carbon transition among different soil and plant carbon pools are shown in Fig. 2. The main functions used in this module are from CLM (Common Land Model) version 5.0 (Lawrence et al., 2019). The dual-porosity framework in the multi-layer soil modelling in Section 2.1 is still applicable for decomposition processes. We do not explicitly label the soil layer and pore region where the variable belongs to.

In BASGRA-BGC model, decomposition is modelled without considering nitrogen stress by assuming sufficient fertilizer input could significantly alleviate nitrogen limitation. Therefore, the carbon fluxes leaving the upstream pools in each soil layer are calculated as:

$$CF_k = \frac{dCP_k}{dt} = CP_k \cdot r_{0,k} \cdot f_{total} \tag{9}$$

The soil respiration, as the CO_2 emissions from the soil, are modelled as:

$$CF_{hr,k} = CF_k \cdot rf_k \tag{10}$$

Meanwhile, as the plant maintenance respiration has not been modelled in the BASGRA_N model, we add the simulation of plant maintenance respiration rate as follows:

$$MR_{sh} = NSH \cdot r_{m,sh} \cdot f_{m,t} \tag{11a}$$

$$MR_{rt} = NRT \cdot r_{m,rt} \cdot f_{m,t} \tag{11b}$$

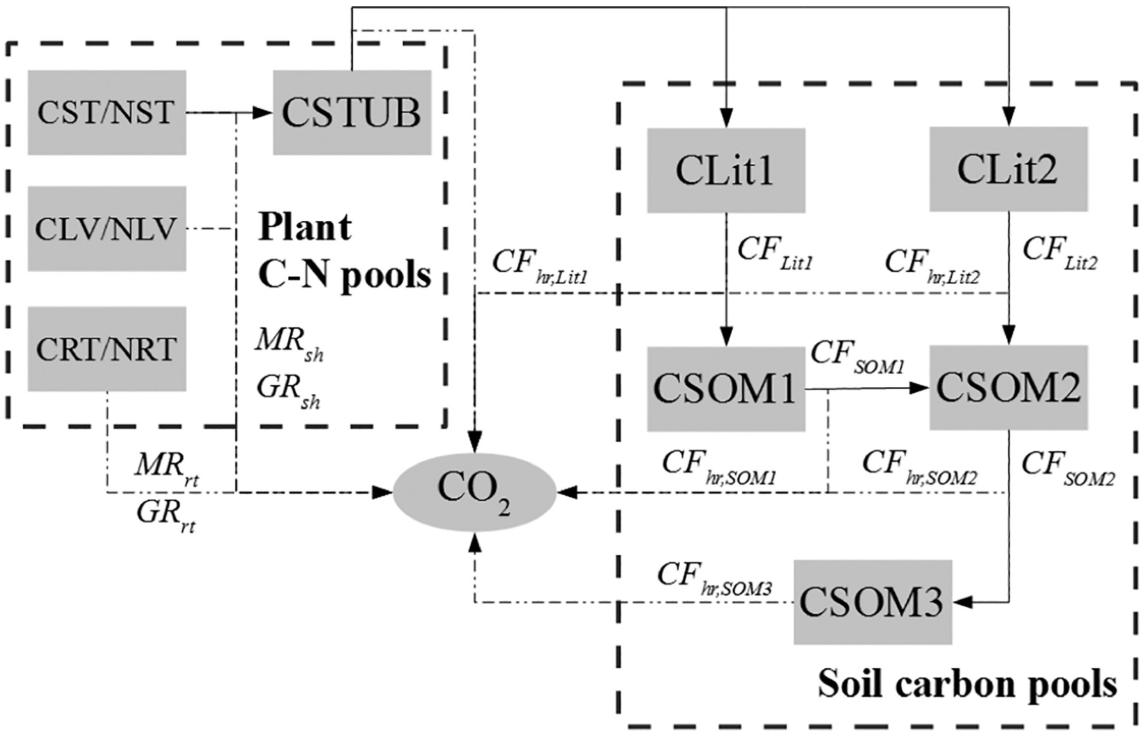

Fig. 2. The pool structure, carbon transition and respiration in the decomposition module of the BASGRA-BGC model (see Table 1 for the explanation of abbreviations).

2.3. Methane modelling

In BASGRA-BGC, we follow DNDC model's routine for CH_4 production (Fumoto et al., 2008) and simplify parts of its functions to simulate the CH_4 production, oxidation and transport processes (see Fig. 3). Hydrogen (H_2) and dissolved organic carbon (DOC) released from root exudation and SOM decomposition are used as electron donors in the reductive reactions of CH_4 production in hydrogenotrophic and acetoclastic methanogenesis, respectively. Thereafter the produced CH_4 is assumed to be transported and emitted to the atmosphere through three main pathways: (i) plants' vascular tissues; (ii) ebullition; (iii) diffusion. Both the atmospheric CH_4 and that produced in deeper soil layers are assumed to be consumed when passing the aerobic zone of soil matrix. The dual-porosity framework in the multi-layer soil modelling in Section 2.1 is still applicable in this CH_4 module.

A simple function based on soil water content is developed to determine the anaerobic fraction in each soil layer:

$$anf = \begin{cases} 0.01, & SW < FC \\ 0.01 + 0.99 \cdot \dfrac{SW - FC}{SAT - FC}, & SW \geq FC \end{cases} \tag{12}$$

The SOM anaerobic decomposition (assumed as Eq. (S13)) rate in each soil layer modelled as:

$$andec_k = CSOM_k \cdot r_{an,k} \cdot f_{total,an} \cdot anf \tag{13}$$

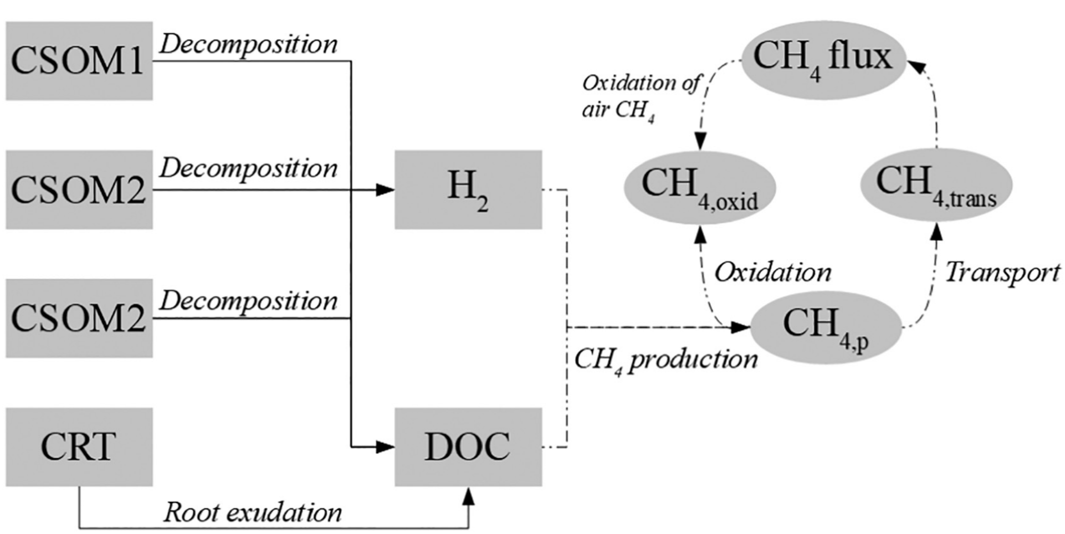

Fig. 3. The schematic description of methane module in the BASGRA-BGC model (see Table 1 for the explanation of abbreviations).

The root exudation process in each soil layer is computed as:

$$RTdec = CRT \cdot r_{RT} \tag{14}$$

As a result, the DOC and H_2 generated in these two processes can be calculated for soil layers. Meanwhile, DOC can be exchanged between mobile and immobile pores and the exchange amount is proportional to the water exchange volume

$$\frac{dDOC}{dt} = RTdec + \sum_{k=1}^{3} \left(andec_k \cdot (1.0 - rf_k)\right) \tag{15a}$$

$$\frac{dH_2}{dt} = \sum_{k=1}^{3} \left(andec_k \cdot 2.0/72.0\right) \tag{15b}$$

The production of CH_4 includes two parts: (i) The reaction of DOC; (ii) The reaction of H_2 and CO_2.

$$CH_{4,p1} = CH_{4,DOC} \cdot \frac{DOC}{km_{DOC} + DOC} \tag{16a}$$

$$CH_{4,p2} = CH_{4,H_2} \cdot \frac{H_2}{km_{H_2} + H_2} \tag{16b}$$

$$CH_{4,p} = CH_{4,p1} + CH_{4,p2} \tag{16c}$$

The CH_4 oxidation is simulated considering the aerobic fraction in each soil layer:

$$CH_{4,oxid} = CH_{4,oxid,\ max} \cdot (1.0 - anf) \cdot f_{total,oxid} \tag{17}$$

The CH_4 transport is modelled using simple linear equation:

$$CH_{4,trans} = CH_{4,p} \cdot \left(f_p + f_e + f_d\right) \tag{18}$$

2.4. Water stress for deficient aeration conditions

Waterlogged conditions in the peat soils could result in the stress of oxygen deficit for root activities and therefore limit grass growth. As such stress is not explicitly modelled in BASGRA_N, we used the simple linear curve as in AquaCrop model (Raes et al., 2012) to simulate the effect of deficient aeration on grass transpiration in Eq. (19). Limited

Fig. 4. The locations of four experiment sites in the Nordic region.

transpiration due to oxygen deficit could further lower the photosynthesis rate following the original procedure of the BASGRA_N model.

$$K_{aer} = \begin{cases} 1.0, & \theta_{rt} < \theta_{air} \\ \frac{\theta_{rt,sat} - \theta_{rt}}{\theta_{rt,sat} - \theta_{air}}, & \theta_{rt} \geq \theta_{air} \end{cases} \tag{19}$$

3. Materials

3.1. Site description

We used observations from four experimental grassland sites on peatlands distributed across the Nordic region to parameterize the model and validate the model performance. The experimental sites Jokioinen, Rovaniemi, Nørreå and Bodø were located in Southern and Northern Finland, Denmark and Northern Norway, respectively (see Fig. 4 for their locations), covering a broad range of climatic conditions spanning from subarctic to temperate and soil properties with a long history of drainage. The general information is listed in Table 2. The main grass species are reed canary grass (*Phalaris arundinacea*) and poa (*Poa spp.*) at Nørreå but timothy (*Phleum pratense*) at other sites. The experiments at the sites Nørreå (Karki et al., 2019) and Bodø (Kløve et al., 2010), included multiple plots with different management treatments. Here we used the measurements from the *control treatment* (poorly drained by ditch) at Nørreå and the *pipe drained plot* at Bodø (other treatments at these two sites are not for drainage practices) for daily-level model validation. Meanwhile, we also used the annual estimations of CH_4 emissions from *flooded treatment* at Nørreå and the *natural plot* at Bodø. The water table fluctuation was monitored continuously during the experimental period by the pressure sensors installed in a perforated PVC tube (Nørreå) or groundwater wells (Bodø) and then the daily averages were used in this study. In Finnish experiments, WTLs were measured periodically in perforated plastic dipwells around the field plots. At all four sites, ER (ecosystem respiration; CO_2) and CH_4 emissions were measured using manual chambers. GPP (gross primary production) measurements were only available in Nørreå. These measurements were carried out periodically at intervals that varied by 7–21 days over the season depending on environmental conditions and timing of management practices (e.g. fertilization, harvest).

Table 2
The information of experimental sites.

Site	Jokioinen[a,b]	Rovaniemi[a,b]	Nørreå[c]	Bodø[d]
Country	Finland	Finland	Denmark	Norway
Coordinate	60°49′N, 23°30′E	66°35′N, 26°01′E	56°27′N, 9°40′E	67°17′N, 14°28′E
Annual precipitation (mm)	607	537	650	1055
Average daily temperature (°C)	4.3	0.0	7.9	4.3
Period	1999.09.01-2002.09.30	2000.05.01-2002.06.30	2015.01.01–2017.03.31	2003.08.09-2004.11.30
Drainage	tile drainage	open ditch drainage	open ditch drainage (control treatment)	tile drainage (P treatment)
Grass species	*Phleum pratense* and *Festuca pratensis*	*Phleum pratense* and *Festuca pratensis*	*Festulolium* and *Tall fescue*	*Phleum pretense* and *Elytrigia repens*
Peat depth (cm)	55	100	83	64
Soil bulk density (g/cm^3)	0.51 (0–20 cm)	0.29 (0–20 cm)	0.33 (0–18 cm); 0.31 (18–45 cm); 0.18 (45–57 cm); 0.15 (57–83 cm);	0.23 (0–24 cm); 0.19 (24–42 cm); 0.15 (42–64 cm)
Organic C (%)	24.0 (0–20 cm)	45 (0–20 cm)	38.6 (0–18 cm); 39.7 (18–45 cm); 45.0 (45–57 cm); 46.9 (57–83 cm);	42.0 (0–24 cm); 44.7 (24–42 cm); 46.6 (42–64 cm);
Total N (%)	1.1 (0–20 cm)	2.5 (0–20 cm)	3.3 (0–18 cm); 3.3 (18–45 cm); 3.1 (45–57 cm); 2.8 (57–83 cm);	2.4 (0–64 cm)
Porosity (%)	71 (0–20 cm)	91 (0–20 cm)	83 (0–18 cm); 83 (18–45 cm); 87 (45–57 cm); 91 (57–83 cm);	83 (0–24 cm); 86 (24–42 cm); 89 (42–64 cm);
Saturated hydraulic conductivity (mm/h)	12 (0–20 cm)	12 (0–20 cm) 3 (20–30 cm) 1 (30–40 cm)	6.4 (0–18 cm); 2.1 (18–45 cm); 1.8 (45–57 cm); 1.4 (57–83 cm);	12 (0–24 cm); 14 (42–64 cm);

[a] Regina et al., 2004.
[b] Regina et al., 2007.
[c] Karki et al., 2019.
[d] Kløve et al., 2010.

3.2. Model forcing data

Daily maximum/minimum temperature, global radiation, precipitation, wind speed and relative humidity are required climatic forcing for model running. We used the in-situ measurements for all these variables at Jokioinen and Bodø sites during the simulating period. For the Rovaniemi site, there were no in-situ records for global radiation. Instead, we used the corresponding measurements from the nearest station (Sodankylä Tähtelä) from the open dataset of the Finnish Meteorological Institute (Weather Observation). For Nørreå site, all the climatic forces are from the national weather station located ca. 5 km from the study site. Other site-specific information needed to drive the model, including peat soil properties (carbon content, porosity, field capacity, wilting point and hydraulic conductivity), management records (harvest date, fertilizer amount) and drainage-related parameters (e.g. the Input in Table 1) were also collected. Soil profile depth (upper peat layer + lower soil layer) was set at 1.5 m and divided into over 15 soil layers according to the detailed soil data (see Table S1). As the measured WTL could drop below the peat soil layer, we assumed the soil texture below the peat soil as loam or sandy soil with low hydraulic conductivity as it is the most common condition for cultivated peatlands.

3.3. Field observations of WTL, CO_2 and CH_4

We validated the daily-step outputs of the BASGRA-BGC model with field measurements including WTL, ER and CH_4 emissions. The primary WTL data was used directly without post-processing. At each site, there were 2–3 replicated plots for the same treatment and 2–3 replicated samplings of ER and CH_4 for each plot and time point. We computed the average emissions per site, treatment and time point and used those for comparison with the corresponding simulated values. We did not interpolate the discontinuous ER and CH_4 flux measurements into daily step to avoid introducing uncertainty with interpolating methods. Instead, we compared the measured values with model outputs on the corresponding measuring day. The ER and CH_4 emissions were usually measured at mid-day for a few hours, and may thus significantly differ from daily averages. Therefore, we corrected measured values of ER to the daily average using the modified van't Hoff equation (Davidson et al., 2006):

$$F_{ave} = F_m \cdot Q_{10}^{((T_{ave}-T_m)/10.0)} \tag{20}$$

where F_{ave} and F_m are the emission rates at daily average temperature T_{ave} and maximum temperature T_m; Q_{10} is the scaling parameter. We assumed that the emission measurements were obtained at the daily maximum temperature and thus used the daily average temperature to correct it with $Q_{10} = 2.0$ (Petersen et al., 2012). We kept the primary CH_4 measurements as its emissions are influenced by more complicated environmental factors.

3.4. Model setup and parameterization

A spin-up running for drained peatlands could bring significant uncertainty to the soil carbon balance as detailed drainage history is usually unavailable. Therefore, for the four sites in this research, we directly ran the model during the experimental period (see Table 2, period). The initial C stocks in $CSOM_1$, $CSOM_2$ and $CSOM_3$ pools accounted for 3, 60 and 37% of the total organic carbon, respectively (see Table S2). As the four sites had been drained for decades, the proportions of immobile and mobile pores in the total porosity were set equally to 50% and 50% (see Table S2). We used the WTL measurement closest to the first running day and then set the initial soil water content in the layers below the water table as saturated and the ones in layers above water table at field capacity. The initial soil temperature across the soil column was set at the air temperature at the first day. Besides, we used two kinds of parameterization schemes (see Table 3): (i) Param1: a set of fixed parameters with commonly used values in other models for all the four sites; and (2) Param2: using site-specific values for part of parameters to account for the difference in peat quality that affects the SOM decomposition potential and grass species that have different tolerances to oxygen deficit and yield potentials. We manually adjusted the parameter values to make the daily observations and simulations better fit. All parameter values and their relevant sources are presented in Table S2.

3.5. Model evaluation

To evaluate the model, we compared the simulated daily WTL, ER and CH_4 emissions with measurements. We used three indicators *RMSE* (Root Mean Square Error), *NRMSE* (Normalized Root Mean Square Error) and *Pearson's r* (Pearson correlation coefficient) to quantify the discrepancy and correlation between simulations and observations for WTL, ER and CH_4. In addition, we aggregated the model daily outputs into annual emission factors and validated the C balance using the estimations from relevant studies for the same sites (labelled in Table 5), including annual GPP, NEE (net ecosystem exchange), SR (soil respiration), ER and grass yield. We also compared the simulated annual emission factors of CH_4 at the four sites with estimations from previous studies (labelled in Table 6) as an additional quality assessment.

4. Results

4.1. Comparison between two parameterization schemes

The model outputs using two parameterizations schemes were compared with daily observations and the values of indictors were

Table 3
The parameterization scheme of the BASGRA-BGC model for the four sites.

Parameter	Unit	Fixed parameter (*Param1*)	Site-specific parameter (*Param2*)			
			Jokioinen	Rovaniemi	Nørreå	Bodø
Parameters in the main text						
$coef_{ex}$	day^{-1}	0.10				
$coef_l$	–	0.70				
D_m	$mm \cdot H_2O/day$	–	–	1.0	0.6	–
D_s	–	–	–	0.38	0.38	–
W_s	–	–	–	0.45	0.45	–
$r_{0,1}$ (Lit_1)	yr^{-1}	4.5				
$r_{0,2}$ (Lit_2)	yr^{-1}	1.4				
$r_{0,3}$ (SOM_1)	yr^{-1}	1.0	0.6	0.7	1.0	0.7
$r_{0,4}$ (SOM_2)	yr^{-1}	0.027	0.03	0.02	0.04	0.02
$r_{0,5}$ (SOM_3)	yr^{-1}	0.0004				
rf_k (k=1, …,5)	–	0.55, 0.45, 0.26, 0.54, 0.88				
$r_{m,sh}$	$g \cdot C/g \cdot N/day$	0.252	0.25	0.25	0.30	0.25
$r_{m,rt}$	$g \cdot C/g \cdot N/day$	0.218	0.20	0.20	0.25	0.20
$r_{an,k}$	yr^{-1}	0.15	0.15	0.16	0.30	0.16
r_{RT}	day^{-1}	0.001	0.001	0.001	0.002	0.001
km_{DOC}	$g \cdot C/m^3$	61.44				
km_{H_2}	$g \cdot H/m^3$	0.0266				
θ_{air}	–	0.85	0.75	0.75	0.90	0.75
Parameters in the supplementary materials						
β_w	–	0.5				
$coef_p$	–	0.7				
$Q_{10,dec}$	–	2.0	2.1	2.6	2.1	2.0
z_τ	m	0.5				
θ_1	–	0.04				
θ_2	–	0.40				
$Q_{10,m}$	–	2.0	2.2	2.0	1.5	2.0
$Q_{10,P}$	–	3.0				
$CH_{4,30}$	$g \cdot C/g \cdot soil/day$	8.5E-5				
$CH_{4,oxid,0}$	$g \cdot C/m^3/day$	0.0008				
$f_{p,max}$	–	0.8				
$f_{e,max}$	–	0.4				
$f_{d,max}$	–	0.1				

Table 4
The evaluation of the daily simulation of the BASGRA-BGC model for the four sites.

	Jokioinen		Rovaniemi		Nørreå		Bodø	
	Param1	Param2	Param1	Param2	Param1	Param2	Param1	Param2
WTL (water table level)								
RMSE (m)	0.06	0.06	0.10	0.10	0.105	0.103	0.11	0.11
NRMSE (%)	15.2	15.1	17.8	17.8	18.7	18.3	14.5	14.5
Pearson's r	0.58	0.60	0.91	0.91	0.62	0.63	0.79	0.79
ER (ecosystem respiration)								
RMSE (gC/m^2/day)	1.50	1.47	1.42	1.22	3.06	2.43	1.44	1.28
NRMSE (%)	13.2	13.0	17.8	15.3	18.3	14.5	21.0	18.6
Pearson's r	0.87	0.88	0.80	0.83	0.83	0.87	0.75	0.76
CH_4								
RMSE (kgC/ha/day)	0.0022	0.002	0.092	0.085	0.293	0.217	0.36	0.33
NRMSE (%)	19.6	19.0	16.5	15.3	25.1	18.6	24.9	21.9
Pearson's r	0.46	0.47	0.31	0.36	0.25	0.33	0.73	0.80

shown in Table 4. The difference between the two approaches for WTL simulation is negligible as we mainly modified the biological-related parameters. However, simulations for ER and CH_4 were effectively improved by Param2 by using site-specific values to account for the heterogeneity in peat quality, grass species, as well as the uncertainty in model structure. We also presented the comparison of these two parameterization schemes for daily average WTL, SR, PR (plant respiration), GPP and CH_4 emissions in Fig. S1. Due to the higher accuracy of Param2, we present results from Param2 for further analysis in 4.2–4.5.

4.2. Simulation of WTL dynamics

We presented observed daily precipitation, temperature, and WTL together with simulated WTL at Jokioinen, Rovaniemi, Nørreå and Bodø in Fig. 5. At Jokioinen (see Fig. 5a), tile drainage was important in maintaining the simulated and observed WTLs at the level of ~ −0.8 m depth. Heavy rainfall events firstly supplemented the water deficit in the upper soil layer and therefore could not immediately raise WTL. As the site was drained down to the underlying silty loam layer with relatively slower hydraulic conductivity than that of the peat layer, the drainage potential was limited also during normal climatic conditions. At the temperate Nørreå site (see Fig. 5c) with comparatively warm temperature in winter, the simulated and observed WTL dynamics were thus mainly controlled by the precipitation and evapotranspiration patterns. The WTL approached soil surface due to constant precipitation input and low drainage rate of the open ditch, although it dropped occasionally to lower level with high evapotranspiration demand and periodic rain-free conditions. The WTL observations and simulations at the two northernmost sites, Rovaniemi and Bodø, had the largest seasonal variability. At the Rovaniemi site (see Fig. 5b) with an open ditch, the soil freezing contributed significantly to the decline of WTL and it was often seen in cold climate. At the Bodø site (see Fig. 5d), the WTL rose to a high level (~−0.15 m) immediately after an intensive precipitation in 2003 and dropped close to the depth of the drainage pipe (~−0.95 m) during a severe summer drought in 2004.

4.3. Simulation of CO_2 emissions

The simulated ER and SR in daily step are presented in Fig. 6 and the simulated GPP and NEE dynamics in Fig. 7. We also compared the simulated and measured GPP at Nørreå in Fig. S2. The simulated ER series generally captured the temporal pattern and magnitude and the simulated SR followed the dynamic of daily temperature except when the WTL was too high (see Fig. 5c, 2016.07–2016.08). The average simulated SR at northernmost site Rovaniemi (0.9 gC/m^2/day) was lower than at Bodø (1.3 gC/m^2/day) and Jokioinen (2.1 gC/m^2/day). The PR simulations (plant respiration; the difference between ER and SR) were mainly affected by the grass growth as PR increased rapidly with grass growth and abruptly dropped after harvest. In the winter, simulated ER and SR generally equaled as PR approximated zero due to lack of green biomass. The daily variation of PR (as well as ER) was greater than that of SR as the radiation force in the Nordic region has a strong daily-level variation due to frequent cloudiness, which significantly affects the modelling of photosynthesis and growth respiration.

We aggregated daily outputs into yearly values and compared the C balance at Jokioinen, Nørreå and Bodø with reported values (see Table 5). The simulated annual SR was at the rate of 500–700 gC/m^2/yr in these sites (the simulated annual SR at Rovaniemi was 330 gC/m^2/yr, but no estimation was found for this site). However, due to the differences in the grass species and soil nutrient condition, the simulated annual GPP in Nørreå (reed canary grass with high biomass) was about 40–100% higher than in Jokioinen and Bodø (timothy with low biomass). As a result, the grassland in Nørreå was a significant carbon sink with simulated annual NEE over 500 gC/m^2/yr and still remained carbon neutral with exported biomass C considered. Jokioinen and Bodø were net carbon sources based on simulated NEE due to the high decomposition rate.

4.4. Simulation of CH_4 emissions

The daily model outputs of CH_4 emissions at the four sites demonstrated that the CH_4 simulations correspond well with the measurements, as well as with the WTL dynamics (Fig. 8). However, in Fig. 8b-d, model outputs failed to capture the emission peaks at these sites. Comparisons of annual emissions for the 'flooded' treatment (WTL constantly at −0.03 m) in Nørreå and the 'natural' condition (tile drainage cancelled) in Bodø are presented in Table 6 alongside with the drainage modelling. This comparison proved good performance of the BASGRA-BGC model in modelling the annual budget of CH_4 dynamics under different managements. At Jokioinen and Bodø with tile drainage, CH_4 emissions were trivial and could even be a sink for atmospheric CH_4. But as the result of Bodø in 'natural' condition shows, the peatlands could still be a significant CH_4 source once drainage is cancelled and WTL raised. At Nørreå with higher WTL and reed canary grass (higher biomass) cultivation, both the 'control' and 'flooded' treatments emitted larger amounts of CH_4 compared to other sites. We attributed the high emissions at this site (especially under 'flooded' treatment) to the rapid decomposition of grass stubble, to root exudation into the SOM in comparatively higher temperatures and to the high nutrient availability. However, the BASGRA-BGC model still underestimated the annual emissions from the Nørreå site during 2016.03–2017.03.

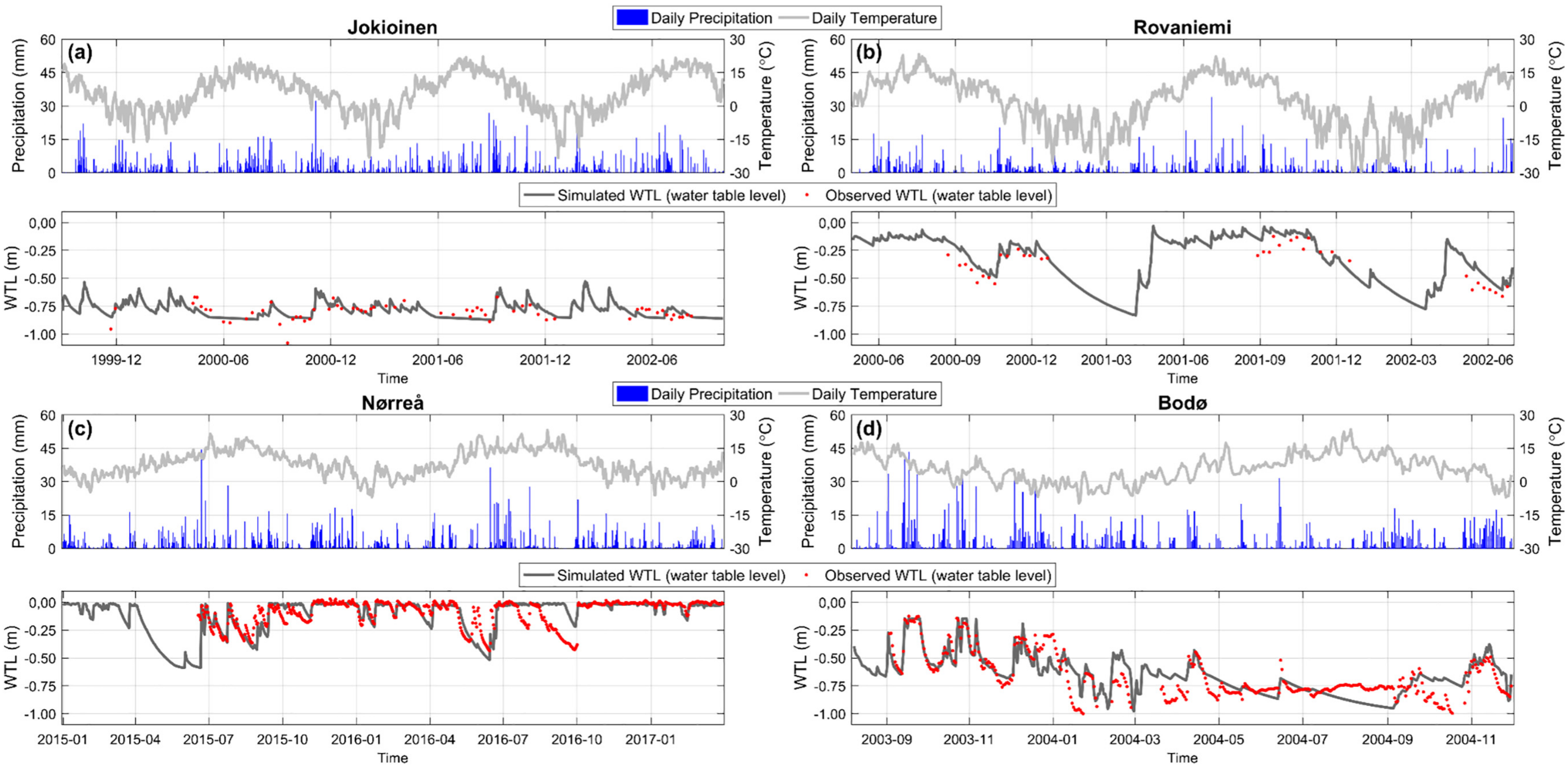

Fig. 5. The climatic conditions and hydrological simulations in the four sites. [WTL: above the soil surface (positive); below the soil surface (negative)].

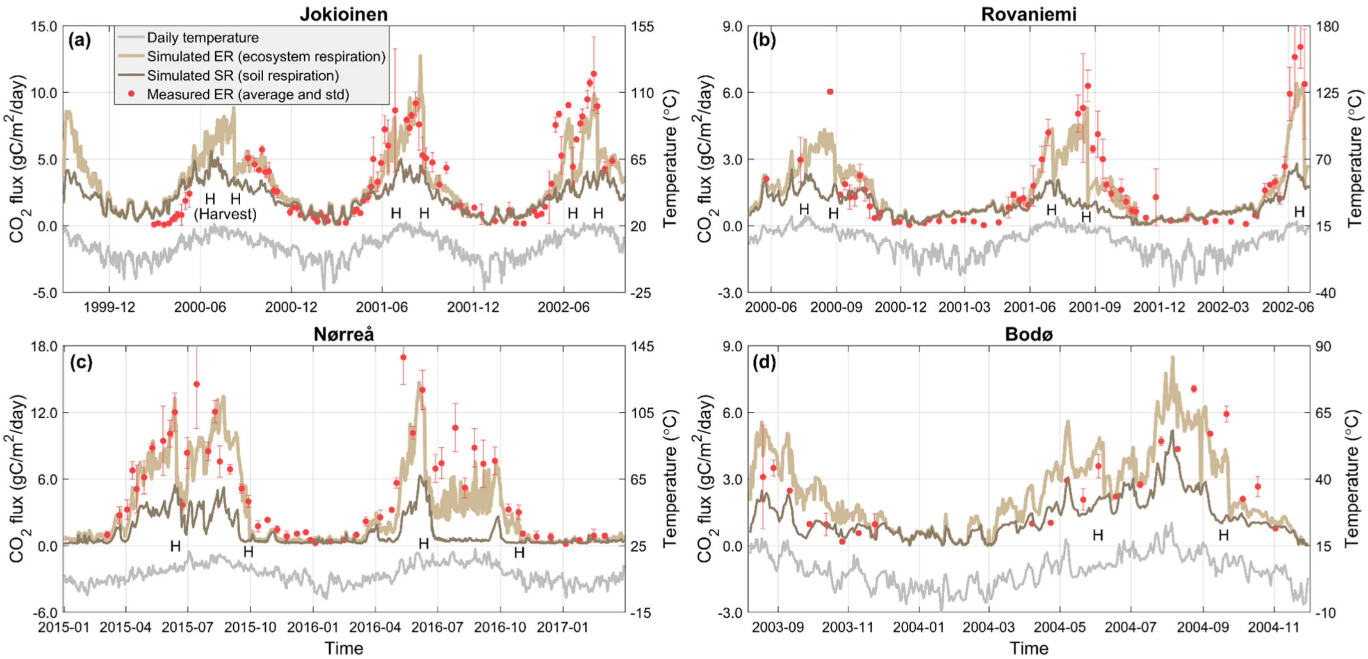

Fig. 6. The simulations of peat decomposition and grass respiration in the four sites. (average and std.: the mean and standard deviation of multiple replicated measurements. The positive value of CO_2 flux means the CO_2 emitted from the soil-plant system into the atmosphere and vice versa.)

4.5. Model application to predict CO_2 and CH_4 emissions and yield as affected by WTL

We used the predictions in Jokioinen during 2000.10–2002.09 to show the potential of the BASGRA-BGC model to provide guidance in improving the WTL management. In this case, we assumed that subsurface irrigation could be applied to rise the average WTL to different levels, under which we predicted the corresponding annual grass yield and CO_2 and CH_4 emissions (see Fig. 9). We used the 100-yr global warming potential value 34 (Myhre et al., 2013) to convert CH_4 emissions into the CO_2 equivalents. In regime I of Fig. 9, grass yield could be maintained and ~200 gCO_2-C m^{-2} yr^{-1} emission reduction could be achieved with WTL rising from −0.8 to −0.4 m. When the WTL was between −0.8 m and −0.6 m, the emission reduction is not obvious as the water table still remained in the silty loam layer. Emission decrease rate accelerated when the WTL was between −0.6 m and −0.4 m and more of the SOC stock was under anaerobic condition. In regime II, the emissions were still reduced by 40 gCO_2-C m^{-2} yr^{-1}, but the grass yield decreased simultaneously. The emission reduction rate decreased due to the balance between decreased CO_2 and increased CH_4. Within this regime, the peatlands were predicted as C sinks with negative CO_2 equivalent. It can be explained by the lower SOC content in the

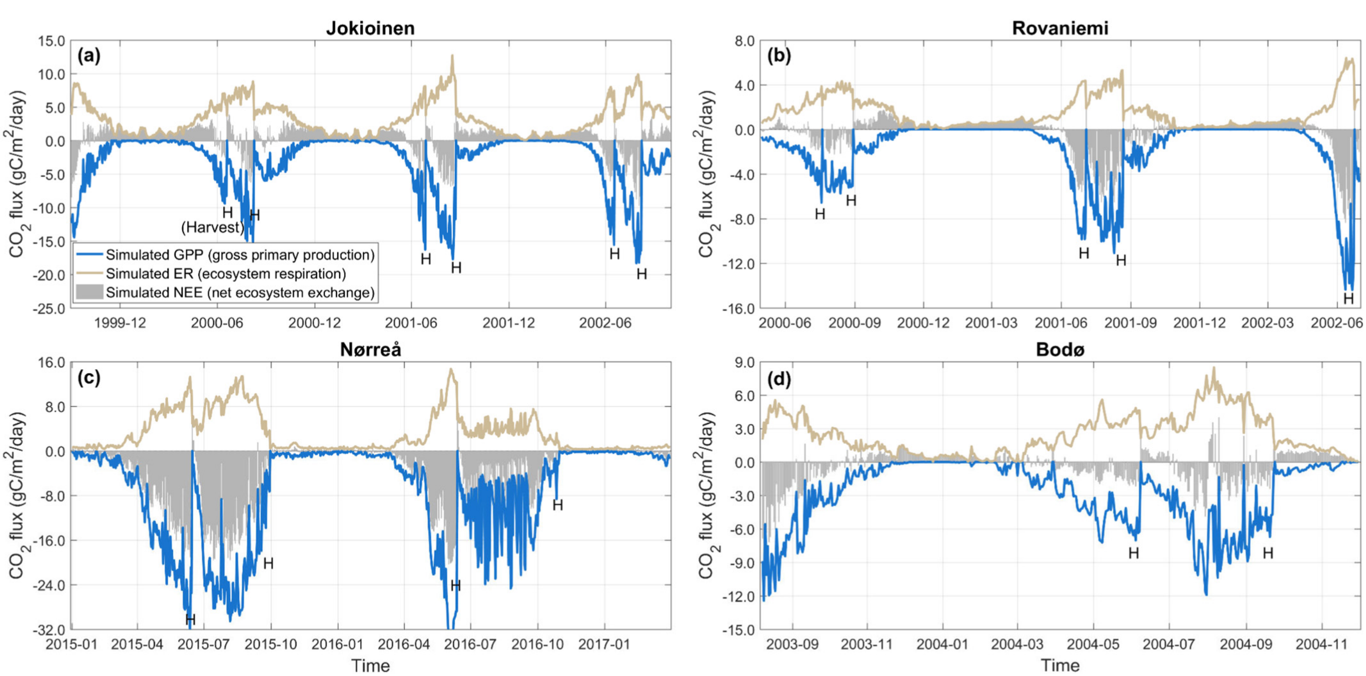

Fig. 7. The simulation of daily GPP, ER and NEE at the four sites. (The positive value of CO_2 flux means the CO_2 emitted from the soil-plant system into the atmosphere and vice versa.)

Table 5
The validation of carbon balance (positive value: carbon lost to the environment; negative value: carbon absorbed from the environment).

	Jokioinen	Nørreå	Bodø
Period	2001.10–2002.09 (annual); 2001.10–2002.03 (winter), 2002.04–2002.09 (summer);	2015.03–2016.02 (Year 1); 2016.03–2017.02 (Year 2);	2003.08.20–2004.11.02
Emission factor of ER (ecosystem resipiration; $gC/m^2/yr$)	Simulated: 1039 (annual)	Literature[c]: 1496 ± 22% (Year 1); 1490 ± 14% (Year 2); Simulated: 1514 (Year 1); 1050 (Year 2);	Literature[e]: 1185–1236 Simulated: 1167
Emission factor of SR (soil respiration; $gC/m^2/yr$)	Literature[a]: 573 ± 245 (annual); 125 ± 71 (winter); 447 ± 145 (summer); Simulated: 659 (annual); 170 (winter); 489 (summer);	Simulated: 589 (Year 1); 353 (Year 2);	Literature[e]: 578–629 Simulated: 609
Annual GPP (gross primary production; $gC/m^2/yr$)	Simulated: −1038 (annual);	Literature[c]: −1973 ± 10% (Year 1); −1862 ± 15% (Year 2); Simulated: −2218 (Year 1); −1595 (Year 2)	Literature[e]: −1012 Simulated: −1034
Annual NEE (net ecosystem exchange; $gC/m^2/yr$)	Literature[b]: 79 ± 25 (annual) Simulated: 36	Simulated: −704 (Year 1); −545 (Year 2)	Literature[e]: 174–225 Simulated: 133
Yield ($gC/m^2/yr$)	Literature[b]: 373 (annual) Simulated: 378 (annual)	Literature[d]: 701 (Year 1); 535 (Year 2); Simulated: 696 (Year 1); 532 (Year 2);	Literature[e]: 405 Simulated: 408
Annual NEE + Exported Yield ($gC/m^2/yr$)	Simulated: 414 (annual)	Simulated: −8 (Year 1); −13 (Year 2);	Literature[e]: 579–640 Simulated: 541

[a] Lohila, 2008.
[b] Lohila et al., 2004.
[c] Karki et al., 2019.
[d] Kandel et al., 2020.
[e] Kløve et al., 2010.

upper peat layer at that site (low SR), and the simulation is for timothy under deficient aeration (low PR) instead of nature vegetation community with high WTL. In regime III with higher WTL, the growth of timothy was greatly limited and the CH_4 production accelerated under the anaerobic condition. The emissions increased unless timothy was replaced by other grass species with high anaerobic tolerance. Based on the model prediction, the current drainage practices with WTL at −0.8 m creates a comfortable zone for grass growth, but had the highest emissions. As a result, we think that a WTL rise up to (~−0.6 m) would be feasible for sustained grass production. Farmers may also take further actions with the help of the model predictions to meet their specific targets.

5. Discussion

5.1. Model performance

We used the dual-porosity framework to simulate the soil moisture under drainage practices for cultivated peatlands. The indicator RMSE demonstrated the “good” performance of WTL modelling with its value less than 15 cm at all the four sites (Mohammadighavam and Kløve, 2016) and it tended to be better than Orchidee-Peat model (24.40–25.93 cm; Qiu et al., 2018). Meanwhile, compared with the empirical methods to calculate ER, the BASGRA-BGC model (0.76–0.88) showed similar (0.71–0.90; Kandel et al., 2013) or even better (0.10; Lohila et al., 2003) skills in terms of r values to capture the temporal dynamics of ER. However, unlike these empirical models that generally target limited variables and need grass-related measurements (e.g. LAI) as inputs, the BASGRA-BGC model could provide more comprehensive outputs including grass growth and soil biogeochemical processes. Meanwhile, the accuracy of the BASGRA-BGC model for cultivated peatlands was also comparable with other process-based biogeochemical models. For example, r values varied between 0.37 and 0.85 and the averaged errors vary between 0.0% and 26% for CH_4 emissions using DNDC model (Deng et al., 2015). Besides, r value was 0.78 and RMSE was 0.83 $gC/m^2/day$ for ER using Orchidee-Peat model (Qiu et al., 2018). Compared with ecological models focusing more on soil biological processes and hydrological model focusing on soil water dynamics, the BASGRA-BGC model showed its advantage on integrating different water management practices and GHG emissions into model simulation. Therefore, it could not only model GHG emissions, but also provide useful predictions to improve the field management.

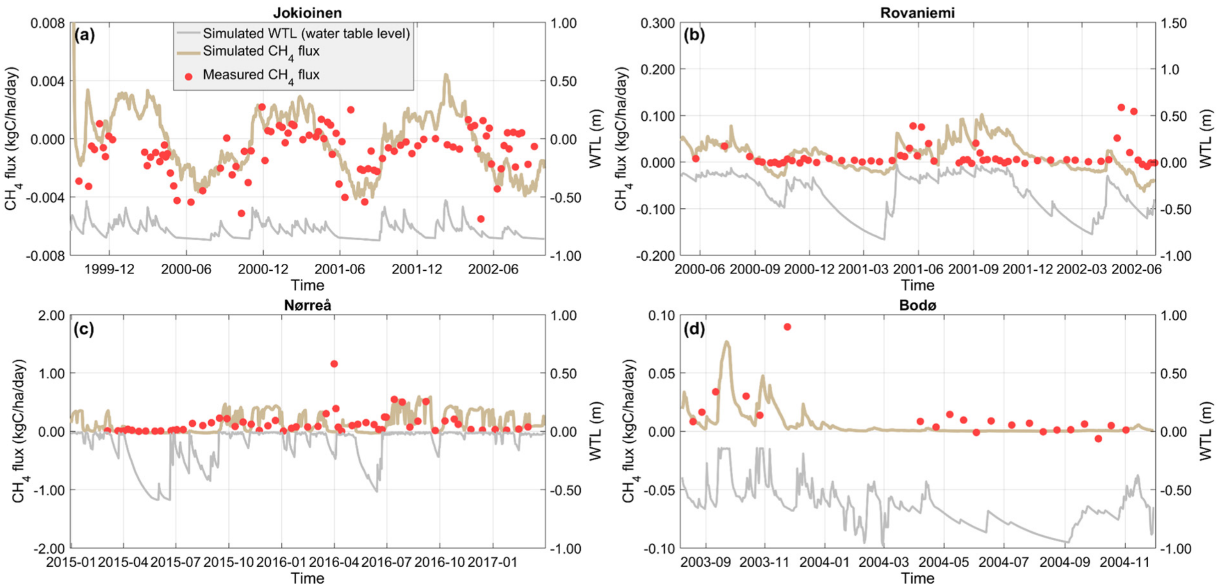

Fig. 8. The daily CH_4 flux at the four sites. (The positive value of CH_4 flux means CH_4 emitted from peat soils and vice versa.)

Table 6
The comparison between simulated annual CH4 flux and estimations.

Site	Period	Simulation (kgC/ha/yr)	Estimation (kgC/ha/yr)
Jokioinen	2000.09–2001.08	−0.14	−0.21 ± 0.18[a]
	2001.09–2002.08	−0.04	−0.20 ± 0.15[a]
Rovaniemi	2000.09–2001.08	3.85	2.73 ± 0.98[a]
Nørreå	2015.03.05–2016.03.04	Control: 31.8 Flooded: 615	Control: 30 ± 25[b] Flooded: 610 ± 170[b]
	2016.03.05–2017.03.04	Control: 68.2 Flooded: 634	Control: 70 ± 30[b] Flooded: 870 ± 130[b]
Bodø	2003.08.20–2004.11.02	Drainage: 2.60 Natural: 43.62	Drainage: 2.06[c] Natural: 48.58[c]

[a] Regina et al., 2007.
[b] Kandel et al., 2020.
[c] Kløve et al., 2010.

Moreover, both the site-specific results and across-site comparison demonstrated negative correlation between SR rates and WTLs and the positive relationship between CH_4 emission rates and WTLs, which corresponded well with the meta-analysis in previous publications (Carlson et al., 2015; Moore and Dalva, 1993; Ojanen et al., 2010). The trade-offs between CO_2 and CH_4 (Hatala et al., 2012) was illustrated in Fig. 9 under different WTLs. The temperature also had significant influence on CO_2 and CH_4 emissions (Lafleur et al., 2005) as both SR and ER were positively correlated with daily temperature (see Fig. 6). All these results guarantee the robustness of our model outputs.

5.2. Uncertainty in observed data

There is inevitable uncertainty in both the measurements to parameterize the model and the input data to drive the model. These uncertainty sources include: (i) As peat soils differ a lot in their quality with respect to the components and drainage history, brief information about total soil C/N contents may not be enough to illustrate the decomposition potential of certain peat soil. Lack of detailed peat quality

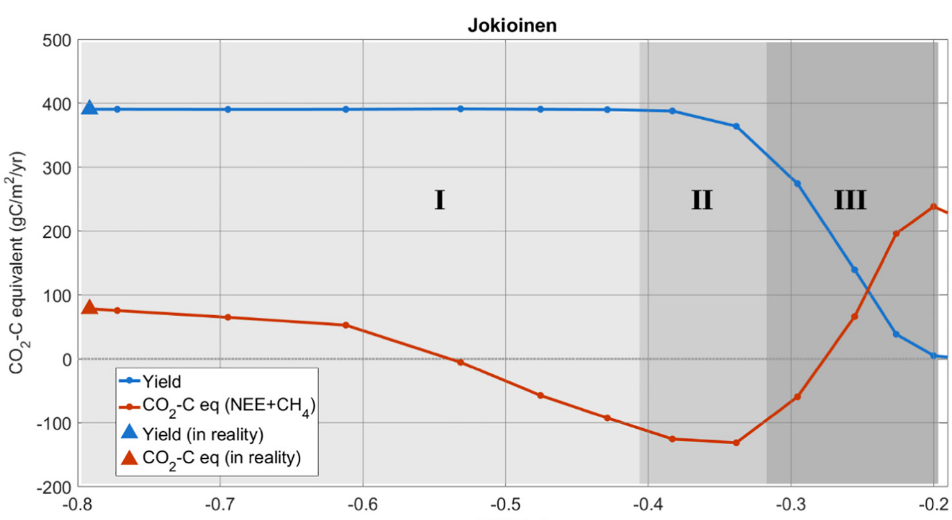

Fig. 9. The simulations of average annual CO_2 equivalents (2000.10–2002-09) for grass yield and GHG emission in Jokioinen under different WTLs.

measurements makes it hard to systemically explain the model parameterization. (ii) The emission measurements with manual chambers have a relatively low sampling frequency. As explained in Section 3.3, the measurements had to be adjusted to daily time step to fit the temporal resolution of model outputs. However, the upscaling method itself introduced uncertainty for model validation. (iii) Direct measurements of SR with similar temporal resolution as ER were not available for any of the four sites. Although we used estimated annual SR rates from previous studies, they were derived either from mass balance calculations or from bare soil measurements, which are both limited in representing the real field conditions. To fully evaluate the model with respect to CO_2 emissions, and the contribution of above- and below-ground processes to the total emissions, more detailed measurements for both SR and ER are needed. The detailed properties in different depths across the soil column will reduce the predictive uncertainty. We expect the continuous measurements (from automatic chambers and eddy covariance) will be available for further validation of model simulations. More accurate approaches to estimate the SR rate from cultivated peatland are needed to determine the loss rate of C stocks.

5.3. Uncertainty in model

The site-specific parameterization scheme (Param2) used for model running was manually determined and therefore subjective and suboptimal. Meanwhile, in the BASGRA-BGC model, decomposition and methane modules focus more on the biological processes of CO_2 and CH_4 production, while the physical transport of the gases especially through the snowpack is not included yet. The simulated ER was systematically overestimated in winter compared with the measurements at Jokioinen, Rovaniemi and Bodø, whereas the model's performance was satisfying at Nørreå with warmer winters (Fig. 6). We believe that the snow cover has a buffering or storing effect on the short-term CO_2 emission pattern but little impact on the annual balance. Besides, most models, including the BASGRA-BGC, do not describe the anaerobic stress for crop growth in detail. To our knowledge, the method used in Section 2.4, as well as other similar methods, are among the few approaches to model the deficient aeration conditions. However, according to the model simulation in Nørreå, the simulated ER and GPP in Year 2 (with higher WTL) had a significant discrepancy from other estimations even though the lower grass yield implies that anaerobic stress indeed existed for grass growth (see Table 4). As a result, a more accurate method for deficient aeration modelling is needed for the waterlogged environment of peat soils. Besides, Nørreå site under flooded condition had greater annual CH_4 emissions in the second year of flooding than in the first year (see Table 5). This indicated that transition period from aerobic and anaerobic conditions should be considered in modelling of CH_4 emissions.

5.4. Implications for field management and research

In Section 4.4, we took Jokioinen as an example to illustrate how the model prediction could be used for decision support to reduce CO_2 and CH_4 emissions and maintain yield. In Fig. 10, we showed the simulated relationship between WTL and SR at the four sites. The corresponding air temperature was divided by 3 °C intervals to minimize the influence of temperature on peat decomposition rate. The results clearly demonstrate that the negative correlation between WTL and SR rate was significant at all sites. However, the within-site variabilities of SR rate among a certain temperature interval reached up to 80%–150% even at the same WTL. Given the small temperature effect, differences in the soil moisture above the water table likely accountable for this diversity. The variation of SR rate was more obvious with deeper WTL as the corresponding soil moisture above became more uncertain compared to shallow WTL. For example, at Jokioinen and Bodø with deep WTL, both short-term drought and heavy precipitation did not induce immediate changes in WTL, but the peat decomposition rate varied greatly due to the fluctuation of soil moisture in the upper SOC-rich layers.

This study proved WTL is still the most important indicator for the balance between climate effects and productivity of cultivated peatlands, which is very operative for monitoring and field management. However, WTL target is most likely insufficient for optimal SOC management when other environmental factors and specific practices are not considered. For instance, to rewet the drained peat soils, surface flooding likely leads to a higher moisture in upper soil layers than

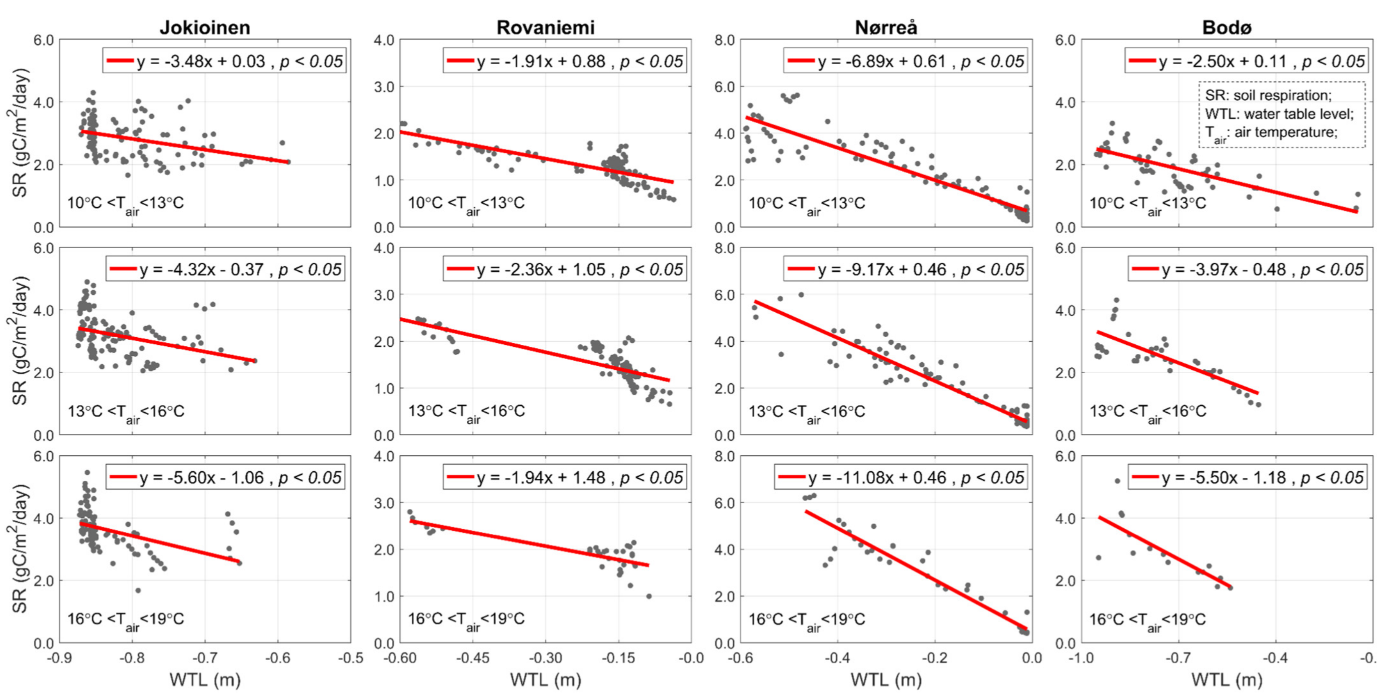

Fig. 10. The relationship between WTL and SR in different temperature intervals.

subsurface irrigation despite of similar WTLs and therefore the two methods would have different peat loss performances. As a result, more indicators and information, including predictions from process-based model, could be used to support developing effective water management practices and decision making. Meanwhile, we suggest that more environmental factors alongside with WTL should be taken into consideration in experimental designs to provide more accurate and objective conclusions about peat carbon balance.

6. Conclusion

The outputs of the BASGRA-BGC model accurately represented the short-term dynamics of WTL, CO_2 and CH_4 emissions, as well as the annual factors for GHG and grass yield. Thereafter, we used the BASGRA-BGC model to predict the effects of WTL control on GHG emissions and grass yield, which demonstrates the strength of such model to improve field management and to balance the production versus the environmental effects. Additionally, the simulations in the four sites indicate that WTL still appears as the most straightforward indicator to prevent C loss from peatlands, but given the significant variability of peat decomposition rate under the same WTL, more environmental factors and information should be considered in accordance with the specific practices. To provide a more comprehensive and accurate assessment of the cultivated peatlands' dynamics, more data with higher temporal resolution across the Nordic region will be collected, and the biogeochemical processes in the BASGRA-BGC model will be further improved in the future work.

CRediT authorship contribution statement

Xiao Huang: Writing – original draft, Methodology, Software, Formal analysis, Visualization. **Hanna Silvennoinen:** Project administration, Funding acquisition, Writing – review & editing. **Bjørn Kløve:** Methodology, Resources, Writing – review & editing. **Kristiina Regina:** Methodology, Resources, Writing – review & editing. **Tanka P. Kandel:** Methodology, Resources, Writing – review & editing. **Arndt Piayda:** Methodology, Resources, Writing – review & editing. **Sandhya Karki:** Methodology, Resources, Writing – review & editing. **Poul Erik Lærke:** Methodology, Resources, Writing – review & editing. **Mats Höglind:** Methodology, Resources, Writing – review & editing.

Declaration of competing interest

The authors declare that they have no known competing financial interests or personal relationships that could have appeared to influence the work reported in this paper.

Acknowledgements

We acknowledge support from the project "Climate smart use of Norwegian organic soils" (MYR, 2017-2022) funded by the Research Council of Norway (decision no. 281109). Thanks go to anonymous reviewers and editor for their constructive comments on this paper. We also thank Dr. Marcel Van Oijen for his valuable suggestions on model development.

Appendix A. Supplementary Information

Supplementary data to this article can be found online at https://doi.org/10.1016/j.scitotenv.2020.144385.

References

Arnold, J.G., Fohrer, N., 2005. SWAT2000: current capabilities and research opportunities in applied watershed modelling. Hydrol. Process. 19 (3), 563–572. https://doi.org/10.1002/hyp.5611.

Berglund, Ö., Berglund, K., 2010. Distribution and cultivation intensity of agricultural peat and gyttja soils in Sweden and estimation of greenhouse gas emissions from cultivated peat soils. Geoderma 154 (3), 173–180. https://doi.org/10.1016/j.geoderma.2008.11.035.

Berglund, Ö., Berglund, K., 2011. Influence of water table level and soil properties on emissions of greenhouse gases from cultivated peat soil. Soil Biol. Biochem. 43 (5), 923–931. https://doi.org/10.1016/j.soilbio.2011.01.002.

Binet, S., Gogo, S., Laggoun-Défarge, F., 2013. A water-table dependent reservoir model to investigate the effect of drought and vascular plant invasion on peatland hydrology. J. Hydrol. 499, 132–139. https://doi.org/10.1016/j.jhydrol.2013.06.035.

Bragazza, L., Buttler, A., Siegenthaler, A., Mitchell, E.A., 2009. Plant litter decomposition and nutrient release in peatlands. Geoph. Monog. 184, 99–110. https://doi.org/10.1029/2008GM000815.

Carlson, K.M., Goodman, L.K., May-Tobin, C.C., 2015. Modeling relationships between water table depth and peat soil carbon loss in southeast Asian plantations. Environ. Res. Lett. 10 (7), 74006. https://doi.org/10.1088/1748-9326/10/7/074006.

Chabbi, A., et al., 2017. Aligning agriculture and climate policy. Nat. Clim. Chang. 7 (5), 307–309. https://doi.org/10.1038/nclimate3286.

Davidson, E.A., Janssens, I.A., Luo, Y., 2006. On the variability of respiration in terrestrial ecosystems: moving beyond Q10. Glob. Chang. Biol. 12 (2), 154–164. https://doi.org/10.1111/j.1365-2486.2005.01065.x.

Deng, J., Li, C., Frolking, S., 2015. Modeling impacts of changes in temperature and water table on C gas fluxes in an Alaskan peatland. Journal of Geophysical Research: Biogeosciences 120 (7), 1279–1295. https://doi.org/10.1002/2014JG002880.

Eickenscheidt, T., Heinichen, J., Drösler, M., 2015. The greenhouse gas balance of a drained fen peatland is mainly controlled by land-use rather than soil organic carbon content. Biogeosciences 12 (17), 5161–5184. https://doi.org/10.5194/bg-12-5161-2015.

Forbord, M., Vik, J., 2017. Food, farmers, and the future: investigating prospects of increased food production within a national context. Land Use Policy 67, 546–557. https://doi.org/10.1016/j.landusepol.2017.06.031.

Franchini, M., Pacciani, M., 1991. Comparative analysis of several conceptual rainfall-runoff models. J. Hydrol. 122 (1), 161–219. https://doi.org/10.1016/0022-1694(91)90178-K.

Frolking, S., Roulet, N.T., Moore, T.R., Richard, P.J.H., Lavoie, M., Muller, S.D., 2001. Modeling northern peatland decomposition and peat accumulation. Ecosystems 4 (5), 479–498. https://doi.org/10.1007/s10021-001-0105-1.

Fumoto, T., Kobayashi, K., Li, C., Yagi, K., Hasegawa, T., 2008. Revising a process-based biogeochemistry model (DNDC) to simulate methane emission from rice paddy fields under various residue management and fertilizer regimes. Glob. Chang. Biol. 14 (2), 382–402. https://doi.org/10.1111/j.1365-2486.2007.01475.x.

Grønlund, A., Hauge, A., Hovde, A., Rasse, D.P., 2008. Carbon loss estimates from cultivated peat soils in Norway: a comparison of three methods. Nutr. Cycl. Agroecosys. 81 (2), 157–167. https://doi.org/10.1007/s10705-008-9171-5.

Harriss, R.C., Gorham, E., Sebacher, D.I., Bartlett, K.B., Flebbe, P.A., 1985. Methane flux from northern peatlands. Nature 315 (6021), 652–654. https://doi.org/10.1038/315652a0.

Hatala, J.A., Detto, M., Sonnentag, O., Deverel, S.J., Verfaillie, J., Baldocchi, D.D., 2012. Greenhouse gas (CO2, CH4, H2O) fluxes from drained and flooded agricultural peatlands in the Sacramento-San Joaquin Delta. Agric. Ecosyst. Environ. 150, 1–18. https://doi.org/10.1016/j.agee.2012.01.009.

Hjelkrem, A.R., Höglind, M., van Oijen, M., Schellberg, J., Gaiser, T., Ewert, F., 2017. Sensitivity analysis and Bayesian calibration for testing robustness of the BASGRA model in different environments. Ecol. Model. 359, 80–91. https://doi.org/10.1016/j.ecolmodel.2017.05.015.

Höglind, M., Van Oijen, M., Cameron, D., Persson, T., 2016. Process-based simulation of growth and overwintering of grassland using the BASGRA model. Ecol. Model. 335, 1–15. https://doi.org/10.1016/j.ecolmodel.2016.04.024.

Höglind, M., Cameron, D., Persson, T., Huang, X., van Oijen, M., 2020. BASGRA_N: a model for grassland productivity, quality and greenhouse gas balance. Ecol. Model. 417, 108925. https://doi.org/10.1016/j.ecolmodel.2019.108925.

Hooghoudt, S.B., 1940. Bijdragen tot de kenins van enige natuurkundige grootheden van de ground. No. 7. Versl. Landbouwk. Onderz [contributions to the knowledge of some physical constants of the soil. No. 7]. Report Agric. Resour. 46, 515–707.

Kandel, T.P., Elsgaard, L., Lærke, P.E., 2013. Measurement and modelling of CO2 flux from a drained fen peatland cultivated with reed canary grass and spring barley. GCB Bioenergy 5 (5), 548–561. https://doi.org/10.1111/gcbb.12020.

Kandel, T.P., Elsgaard, L., Lærke, P.E., 2017. Annual balances and extended seasonal modelling of carbon fluxes from a temperate fen cropped to festulolium and tall fescue under two-cut and three-cut harvesting regimes. GCB Bioenergy 9 (12), 1690–1706. https://doi.org/10.1111/gcbb.12424.

Kandel, T.P., Karki, S., Elsgaard, L., Labouriau, R., Lærke, P.E., 2020. Methane fluxes from a rewetted agricultural fen during two initial years of paludiculture. Sci. Total Environ. 713, 136670. https://doi.org/10.1016/j.scitotenv.2020.136670.

Karki, S., Kandel, T.P., Elsgaard, L., Labouriau, R., Lærke, P.E., 2019. Annual CO_2 fluxes from a cultivated fen with perennial grasses during two initial years of rewetting. Mires & Peat 25. doi:10.19189/MaP.2017.DW.322.

Kasimir, Å., He, H., Coria, J., Nordén, A., 2018. Land use of drained peatlands: greenhouse gas fluxes, plant production, and economics. Glob. Chang. Biol. 24 (8), 3302–3316. https://doi.org/10.1111/gcb.13931.

Kirkham, D., 1957. Theory of Land Drainage. Drainage of agricultural lands. American Society of Agronomy Madison, Wisconsin, In, pp. 139–181.

Kleinen, T., Brovkin, V., Schuldt, R.J., 2012. A dynamic model of wetland extent and peat accumulation: results for the Holocene. Biogeosciences 9 (1), 235–248. https://doi.org/10.5194/bg-9-235-2012.

Kløve, B., Sveistrup, T.E., Hauge, A., 2010. Leaching of nutrients and emission of greenhouse gases from peatland cultivation at Bodin, Northern Norway. Geoderma 154 (3), 219–232. https://doi.org/10.1016/j.geoderma.2009.08.022.

Kløve, B., Berglund, K., Berglund, Ö., Weldon, S., Maljanen, M., 2017. Future options for cultivated Nordic peat soils: can land management and rewetting control

greenhouse gas emissions? Environ. Sci. Pol. 69, 85–93. https://doi.org/10.1016/j.envsci.2016.12.017.
Korhonen, P., et al., 2018. Modelling grass yields in northern climates - a comparison of three growth models for timothy. Field Crop Res. 224, 37–47. https://doi.org/10.1016/j.fcr.2018.04.014.
Lafleur, P.M., Moore, T.R., Roulet, N.T., Frolking, S., 2005. Ecosystem respiration in a cool temperate bog depends on peat temperature but not water table. Ecosystems 8 (6), 619–629. https://doi.org/10.1007/s10021-003-0131-2.
Lawrence, D. et al., 2019. CLM5 documentation. Tech. rep., Boulder, CO: National Center for Atmospheric Research.
Leifeld, J., Menichetti, L., 2018. The underappreciated potential of peatlands in global climate change mitigation strategies. Nat. Commun. 9 (1), 1071. https://doi.org/10.1038/s41467-018-03406-6.
Lloyd, J., Taylor, J.A., 1994. On the temperature dependence of soil respiration. Funct. Ecol. 8 (3), 315–323. https://doi.org/10.2307/2389824.
Lohila, A., 2008. Carbon dioxide exchange on cultivated and afforested boreal peatlands, Finnish Meteorological Institute Contributions 73, Yliopistopaino, Helsinki. PhD Thesis.
Lohila, A., Aurela, M., Regina, K., Laurila, T., 2003. Soil and total ecosystem respiration in agricultural fields: effect of soil and crop type. Plant Soil 251 (2), 303–317. https://doi.org/10.1023/A:1023004205844.
Lohila, A., Aurela, M., Tuovinen, J., Laurila, T., 2004. Annual CO2 exchange of a peat field growing spring barley or perennial forage grass. Journal of Geophysical Research: Atmospheres 109 (D18). https://doi.org/10.1029/2004JD004715.
Maljanen, M., Liikanen, A., Silvola, J., Martikainen, P.J., 2003. Methane fluxes on agricultural and forested boreal organic soils. Soil Use Manag. 19 (1), 73–79. https://doi.org/10.1111/j.1475-2743.2003.tb00282.x.
Mezbahuddin, M., Grant, R.F., Flanagan, L.B., 2016. Modeling hydrological controls on variations in peat water content, water table depth, and surface energy exchange of a boreal western Canadian fen peatland. Journal of Geophysical Research: Biogeosciences 121 (8), 2216–2242. https://doi.org/10.1002/2016JG003501.
Mohammadighavam, S., Kløve, B., 2016. Evaluation of DRAINMOD 6.1 for hydrological simulations of peat extraction areas in northern Finland. J. Irrig. Drain. Eng. 142 (11), 4016053. doi:https://doi.org/10.1061/(ASCE)IR.1943-4774.0001086.
Moore, T.R., Dalva, M., 1993. The influence of temperature and water table position on carbon dioxide and methane emissions from laboratory columns of peatland soils. J. Soil Sci. 44 (4), 651–664. https://doi.org/10.1111/j.1365-2389.1993.tb02330.x.
Myhre, G., et al., 2013. Anthropogenic and Natural Radiative Forcing. Climate Change 2013: The Physical Science Basis. Contribution of Working Group I to the Fifth Assessment Report of the Intergovernmental Panel on Climate Change, 659–740. Cambridge University Press, Cambridge.
Myllys, M., Lilja, H., Regina, K., 2012. The Area of Cultivated Organic Soils in Finland According to GIS Datasets, Proceedings of the 14th International Peat Congress. Peatlands in Balance, Stockholm, Sweden.
Nielsen, O., et al., 2013. Denmark's National Inventory Report 2013: Emission Inventories 1990–2011-Submitted under the United Nations Framework Convention on Climate Change and the Kyoto Protocol Aarhus Universitet (DCE-Nationalt Center for Miljø og Energi).
Ojanen, P., Minkkinen, K., Alm, J., Penttilä, T., 2010. Soil–atmosphere CO2, CH4 and N2O fluxes in boreal forestry-drained peatlands. Forest Ecol. Manag. 260 (3), 411–421. https://doi.org/10.1016/j.foreco.2010.04.036.
Parton, W.J., 1996. The CENTURY model. In: Powlson, D.S., Smith, P., Smith, J.U. (Eds.), Springer. Berlin Heidelberg, Berlin, Heidelberg, pp. 283–291 https://doi.org/10.1007/978-3-642-61094-3_2.
Petersen, S.O., et al., 2012. Annual emissions of CH_4 and N_2O, and ecosystem respiration, from eight organic soils in Western Denmark managed by agriculture. Biogeosciences 9 (1), 403–422. https://doi.org/10.5194/bg-9-403-2012.
Qiu, C., et al., 2018. ORCHIDEE-PEAT (revision 4596), a model for northern peatland CO2, water, and energy fluxes on daily to annual scales. Geosci. Model Dev. 11 (2), 497–519. https://doi.org/10.5194/gmd-11-497-2018.
Qiu, C., et al., 2019. Modelling northern peatland area and carbon dynamics since the Holocene with the ORCHIDEE-PEAT land surface model (SVN r5488). Geosci. Model Dev. 12 (7), 2961–2982. https://doi.org/10.5194/gmd-12-2961-2019.
Raes, D., Steduto, P., Hsiao, T.C., Fereres, E., 2012. AquaCrop Version 4.0: Chapter 3 Calculation Procedures, FAO. Land and Water Division, Rome, Italy.
Regina, K., Alakukku, L., 2010. Greenhouse gas fluxes in varying soils types under conventional and no-tillage practices. Soil Tillage Res. 109 (2), 144–152. https://doi.org/10.1016/j.still.2010.05.009.
Regina, K., Syväsalo, E., Hannukkala, A., Esala, M., 2004. Fluxes of N2O from farmed peat soils in Finland. Eur. J. Soil Sci. 55 (3), 591–599. https://doi.org/10.1111/j.1365-2389.2004.00622.x.
Regina, K., Pihlatie, M., Esala, M., Alakukku, L., 2007. Methane fluxes on boreal arable soils. Agric. Ecosyst. Environ. 119 (3), 346–352. https://doi.org/10.1016/j.agee.2006.08.002.
Rezanezhad, F., Price, J.S., Quinton, W.L., Lennartz, B., Milojevic, T., Van Cappellen, P., 2016. Structure of peat soils and implications for water storage, flow and solute transport: a review update for geochemists. Chem. Geol. 429, 75–84. https://doi.org/10.1016/j.chemgeo.2016.03.010.
Shi, X., et al., 2015. Representing northern peatland microtopography and hydrology within the community land model. Biogeosciences 12 (21), 6463–6477. https://doi.org/10.5194/bg-12-6463-2015.
Smith, L.C., et al., 2004. Siberian peatlands a net carbon sink and global methane source since the early holocene. Science 303 (5656), 353. https://doi.org/10.1126/science.1090553.
Van Oijen, M., Höglind, M., 2016. Toward a Bayesian procedure for using process-based models in plant breeding, with application to ideotype design. Euphytica 207 (3), 627–643. https://doi.org/10.1007/s10681-015-1562-5.
Wania, R., Ross, I., Prentice, I.C., 2009. Integrating peatlands and permafrost into a dynamic global vegetation model: 1. Evaluation and sensitivity of physical land surface processes. Global Biogeochem. Cy. 23 (3). https://doi.org/10.1029/2008GB003412.
Weather observation. Finnish Meteorological Institute. https://en.ilmatieteenlaitos.fi/download-observations.
Wiréhn, L., 2018. Nordic agriculture under climate change: a systematic review of challenges, opportunities and adaptation strategies for crop production. Land Use Policy 77, 63–74. https://doi.org/10.1016/j.landusepol.2018.04.059.
Woodward, S.J.R., Van Oijen, M., Griffiths, W.M., Beukes, P.C., Chapman, D.F., 2020. Identifying causes of low persistence of perennial ryegrass (Lolium perenne) dairy pasture using the Basic Grassland model (BASGRA). Grass Forage Sci. 75 (1), 45–63. https://doi.org/10.1111/gfs.12464.
Yu, Z.C., 2012. Northern peatland carbon stocks and dynamics: a review. Biogeosciences 9 (10), 4071–4085. https://doi.org/10.5194/bg-9-4071-2012.